
Article:
Newsome, B. and Evans, M. orcid.org/0000-0003-4775-032X (2017) Impact of uncertainties in inorganic chemical rate constants on tropospheric composition and ozone radiative forcing. Atmospheric Chemistry and Physics. pp. 14333-14352. ISSN 1680-7324

https://doi.org/10.5194/acp-2017-12

Atmos. Chem. Phys. Discuss., doi:10.5194/acp-2017-12, 2017
Manuscript under review for journal Atmos. Chem. Phys.
Discussion started: 9 March 2017

Atmospheric Chemistry and Physics Discussions

Impact of uncertainties in inorganic chemical rate constants on tropospheric composition and ozone radiative forcing

Ben Newsome[1] and Mat Evans[1,2]

[1]Wolfson Atmospheric Chemistry Laboratories, Department of Chemistry, University of York, York, YO10 5DD, UK.
[2]National Centre for Atmospheric Science, Department of Chemistry, University of York, York, YO10 5DD, UK.

Correspondence to: Mat Evans (Mat.Evans@york.ac.uk)

Abstract. Chemical rate constants determine the composition of the atmosphere and how this composition has changed over time. They are central to our understanding of climate change and air quality degradation. Atmospheric chemistry models, whether online or offline, box, regional or global use these rate constants. Expert panels synthesise laboratory measurements, making recommendations for the rate constants that should be used. This results in very similar or identical rate constants being used by all models. The inherent uncertainties in these recommendations are, in general, therefore ignored. We explore the impact of these uncertainties on the composition of the troposphere using the GEOS-Chem chemistry transport model. Based on the JPL and IUPAC evaluations we assess 50 mainly inorganic rate constants and 10 photolysis rates, through simulations where we increase the rate of the reactions to the 1 σ upper value recommended by the expert panels.

We assess the impact on 4 standard metrics: annual mean tropospheric ozone burden, surface ozone and tropospheric OH concentrations, and tropospheric methane lifetime. Uncertainty in the rate constants for NO_2 + OH $\xrightarrow{M}$ HNO_3, OH + CH_4 $\rightarrow$ CH_3O_2 + H_2O and O_3 + NO $\rightarrow$ NO_2 + O_2 are the three largest source of uncertainty in these metrics. We investigate two methods of assessing these uncertainties, addition in quadrature and a Monte Carlo approach, and conclude they give similar outcomes. Combining the uncertainties across the 60 reactions, gives overall uncertainties on the annual mean tropospheric ozone burden, surface ozone and tropospheric OH concentrations, and tropospheric methane lifetime of 11, 12, 17 and 17% respectively. These are larger than the spread between models in recent model inter-comparisons. Remote regions such as the tropics, poles, and upper troposphere are most uncertain. This chemical uncertainty is sufficiently large to suggest that rate constant uncertainty should be considered when model results disagree with measurement.

Calculations for the pre-industrial allow a tropospheric ozone radiative forcing to be calculated of 0.412 $\pm$ 0.062 Wm^{-2}. This uncertainty (15 %) is comparable to the inter-model spread in ozone radiative forcing found in previous model-model inter-comparison studies where the rate constants used in the models are all identical or very similar. Thus the uncertainty of tropospheric ozone radiative forcing should expanded to include this additional source of uncertainty. These rate constant uncertainties are significant and suggest that refinement of supposedly well known chemical rate constants should be considered alongside other improvements to enhance our understanding of atmospheric processes.

Atmos. Chem. Phys. Discuss., doi:10.5194/acp-2017-12, 2017
Manuscript under review for journal Atmos. Chem. Phys.
Discussion started: 9 March 2017

Atmospheric Chemistry and Physics Discussions

1 Introduction

The concentration of gases and aerosols in the atmosphere have changed over the last century due to human activity. This has resulted in a change in climate (Stocker, 2014) and a degradation in air quality (Dockery et al., 1993) with tropospheric ozone (O_3) and methane (CH_4) playing a central role. The response of these compounds to the changing emissions is complex and non-linear (Lin et al., 1988). The hydroxyl radical (OH) plays a central role in this chemistry as it initiates the destruction of many pollutants (notably CH_4) and so determines their lifetime in the atmosphere. The dominant source of OH is the photolysis of O_3 in the presence of water vapour. The oxidation of compounds such as CH_4, carbon monoxide (CO) and other hydrocarbons can lead to the production of O_3 if sufficient oxides of nitrogen (NO_x) are present. Changes in the emissions of O_3 precursors between the pre-industrial ($\sim$1850) and the present day have increased O_3 concentrations and this has produced a radiative forcing estimated to be 410 ± 65 mWm^{-2} (Stevenson et al., 2013).

The rate constants of the reactions occurring in the atmosphere have been determined by a number of laboratory studies which are synthesised by groups such as the IUPAC (Atkinson et al., 2004) and JPL (Sander et al., 2011) panels. These provide recommendations for both rate constants and their associated uncertainties. These reactions are typically expressed in an Arrhenius form to represent the temperature dependence. More complicated representations are needed for three-body reactions. The 1σ uncertainty in a rate constant at a temperature (T) is expressed as an uncertainty at 298K (f (298)) together with a term (g) that expresses how quickly the uncertainty increases away from 298K (Equation 1), leading to temperature dependences which increase away from room temperature (Figure 1).

$$f(\mathrm{T}) = \mathrm{f}(298\mathrm{K}) \exp\left|g\left(\frac{1}{\mathrm{T}} - \frac{1}{298\mathrm{K}}\right)\right| \quad (1)$$

For the reactions studied, the uncertainty at 298K typically ranges from 5% for well understood reactions to 30% for those which have significant uncertainty. Other reactions can have larger uncertanties then quoted here. The increase in uncertainty at temperatures away from 298K can range from 0% to over 40%, giving some reactions a total uncertainty of over 50% in the cold upper troposphere.

Models of atmospheric composition (whether online or offline, single box or transport etc.) use these recommended rate constants, together with estimates of the meteorology, emissions, deposition, photolysis, etc. of compounds to calculate the concentration of species in the atmosphere. These models are a central tool for our understanding of atmospheric processes and for making policy choices to minimize climate change and air pollution.

Although these models have been developed significantly over the last decades, they have, in general, all used the same basic chemical rate constants as evaluated by the IUPAC or JPL panels. Little emphasis has been placed on understanding the uncertainty in predicted atmospheric composition caused by the uncertainty in these rate constants. The focus has been to investigate the impacts of novel chemical reactions, understanding emissions etc. (e.g. (Sherwen et al., 2016; Hartley and Prinn, 1993)). Here though, we investigate the impact of this uncertainty on the composition of the troposphere. We base our assessment on the uncertainties in rate constants described by the JPL and IUPAC panels (Sander et al., 2011; Atkinson et al., 2004) using the GEOS-Chem model and evaluate a range of model diagnostics for both the present day and the pre-industrial.

Atmos. Chem. Phys. Discuss., doi:10.5194/acp-2017-12, 2017
Manuscript under review for journal Atmos. Chem. Phys.
Discussion started: 9 March 2017

Atmospheric Chemistry and Physics Discussions

2 Model simulations

GEOS-Chem (Bey et al., 2001) (www.goes-chem.org) is an offline chemistry transport model. We use version v9-2. For computational expediency we use a horizontal resolution of 4° latitude by 5° longitude with 47 vertical hybrid pressure-sigma levels from the surface to 0.01 hPa. The chemistry is solved within the troposphere with the SMV-Gear solver (Jacobson and Turco, 1994). We use a mass based scheme for aerosol (Park et al., 2003) and so can not investigate the impact of the rate constant uncertainty on aerosol number or size distribution. Stratospheric chemistry is unchanged in all simulations and uses a linearised approach to the chemistry (McLinden et al., 2000; Murray et al., 2012). Global anthropogenic emissions were taken from the Emission Database for Global Atmospheric Research (EDGAR) v3 for NOx, CO,VOCs and SOx. Regional or source specific inventories replaced EDGAR where appropriate (EMEP, BRAVO, Streets, CAC, NEI05, RETRO, AEIC see the GEOS-Chem wiki for more details). Biogenic emissions (Isoprene, Monoterpenes, Methyl Butenol) are taken from the MEGAN v2.1 emission inventory (Sindelarova et al., 2014). Biomass burning emissions were used from the GFED3 monthly emission inventory(van der Werf et al., 2010). NO_x sources from lightning (Murray et al., 2012) and soils (Hudman et al., 2012) were also included. As in previous studies (Parrella et al., 2012; Sofen et al., 2011) pre-industrial emissions are calculated by switching off anthropogenic emissions, reducing biomass burning emissions to 10% of their modern day values, and by setting CH_4 concentrations to a constant 700 ppbv (Parrella et al., 2012).

For both present-day and the pre-industrial simulations we run the model from the 1st of July 2005 to the 1st of July 2007 with GEOS-5 meteorology. We used the first year to spin up the composition of the troposphere. Metrics are derived from the second year of simulation.

We follow the methodology of JPL (Sander et al., 2011) for the representation of uncertainties in rate constants. For two body reactions the uncertainty is given by two parameters. f (298K) describes the relative uncertainty at 298K, and g describes how the uncertainty increases as temperature diverges from 298K, as shown in equation (1).

3 Reactions Studied

We limit our study to the inorganic (O_x, HO_x, NO_x, CO, CH_4) reactions together with some key organic and sulfur reactions. Mechanistic uncertainties in the organic chemistry of the atmosphere makes a systematic assessment of these uncertainties difficult (Goldstein and Galbally, 2007). Table 1 shows a list of reactions that are perturbed and the uncertainties assumed. We use the uncertainty recommendations from the JPL panel if provided and the IUPAC panel otherwise. We investigate the impact of 50 inorganic chemical reactions and 10 photolysis reactions (Table 1). Uncertainties in photolysis rate constants are harder to define than for the other reactions. We consider the appropriate chemical uncertainty here as the uncertainty in the absorption cross section and the quantum yield rather than the uncertainty in the photon flux which we attribute to the radiative transfer calculation. A full calculation of the chemical uncertainty in a photolysis rate is complex as it it depends upon the uncertainties at different wavelengths, the independence of the cross section and quantum yield parameters and the transfer of this information through the spectral bins used for the laboratory studies and the photolysis calculations. In order to simplify this calculation we apply a 10% uncertainty to all photolysis rates.

Atmos. Chem. Phys. Discuss., doi:10.5194/acp-2017-12, 2017
Manuscript under review for journal Atmos. Chem. Phys.
Discussion started: 9 March 2017

Atmospheric Chemistry and Physics Discussions

4 Single Reaction Perturbations

From each of these 60 reactions we increase the reaction rate by the 1 σ temperature dependent uncertainty given in Table 1. To allow the model to spin up we take the 2nd year of simulation and calculate four metrics: tropospheric O_3 burden, mean surface O_3 mixing ratio, tropospheric mass weighted mean OH number density, and tropospheric mean CH_4 lifetime. We subtract the values of these metrics from the base value of the metric (unchanged rate constants) and then take the absolute value to remove cases where the value decreases on an increase in the rate constant. Figure 2 shows the changes for all four metrics with Table 1 giving the values for the change in tropospheric O_3 burden. We express these values as a percentage of the base case value.

It is evident that a relatively small number of reactions produce large uncertainties in the values of these metrics. The one that offers the most uncertainty is the reaction between NO_2 and OH to product nitric acid which leads to uncertainties in the range of 6–11% in the metrics investigated here. This reaction is both highly uncertain (f (298K)=30%) and acts as a large global sink for NO_x and HO_x. The next most significant reaction is that between CH_4 and OH to produce CH_3O_2 radicals. The model assumes a constant CH_4 concentration so an increase in the rate constant between CH_4 and OH leads to an increased source of radicals but doesn't lead to a commensurate drop in the CH_4 concentration. Thus an increase in this rate constant in the model is effectively the same as an increase in the emission of CH_4 which results in a wide range of impacts such as increased CO concentrations etc. The O_3+NO reaction to produce NO_2 is central to the partitioning of NO_x in the atmosphere. Thus increasing its rate constant reduces NO concentrations in the atmosphere (leading to lower O_3 concentrations) and increasing the concentration of NO_2 (which favours NO_2 removal) which again reduces O_3 concentrations. The tenth most significant reaction for all the metrics generates an uncertainty of less than 1%.

The relative importance of the different reactions does not change much with the metric being investigated (see Figure 2). The rate constants of these top ten reactions are not particularly uncertain (other than for NO_2+OH) compared to other reactions but they link important chemical cycles and have a very large chemical flux flowing through them. Thus relatively small changes in their uncertainties will lead to large changes in concentration.

Given the uncertainties for the individual reactions calculated here, the next question is as to how these uncertainties can be combined together to generate a single uncertainty from rate constants uncertainty on the composition of the atmosphere.

5 Addition of uncertainties

If these perturbations are independent (uncertainties in one rate constant are not related to uncertainties in another) and the model approximately linear, the total rate constant uncertainty can be found by finding the root of the sum of the individual uncertainties squared (addition in quadrature) as shown in equation (2).

$$\sigma^2_{total} = \Sigma\sigma^2_{reaction} \tag{2}$$

Atmos. Chem. Phys. Discuss., doi:10.5194/acp-2017-12, 2017
Manuscript under review for journal Atmos. Chem. Phys.
Discussion started: 9 March 2017

Atmospheric Chemistry and Physics Discussions

It is hard to assess the independence of the rate constants. Given the nature of the laboratory experiments used to determine them, it is likely that there is some overlap in assumptions. It would be extremely difficult to diagnose this for all 60 reactions and so we ignore this in further work.

Atmospheric chemistry is non-linear (Lin et al., 1988). A doubling of a change to the model, does not necessarily lead to a doubling of the model response. Thus, is it not obvious how uncertainties from the individual rate-constant perturbations should be combined. To investigate this we perform a Monte Carlo analysis of the model. We take ten of the most significant reactions determined earlier (shown by the * in Table 1) and generate 10 normally distributed random numbers ($\mu = 0$, σ=1), one for each reaction. For each of the ten rate constants we add on the calculated 1σ uncertainty multiplied by the random number and run the model. We repeat this 50 times to produce a Monte-Carlo ensemble from which we can calculate the four metrics described earlier.

If the model is linear, the metrics calculated from each member of the Monte Carlo ensemble should be (to some level) the same as the linear addition of the individual rate-constant perturbations weighted by the Monte Carlo random numbers. Figure 3 shows the perturbation in the value of the metric calculated for each ensemble member against the calculated value of the metric using the single reaction values. The model shows a strong linear relationship between the metrics examined (intercepts of 0.21 ± 0.9 % and gradients of 0.80 ± 0.04) thus if the errors are uncorrelated we can, at least to a first approximation, add the individual 1σ perturbations together in quadrature using Equation 2 to calculate the overall uncertainty in the model metrics. From these simulations we estimate the quadrature approach leads to an over-estimate of the 1σ uncertainty on the order of 10%.

We thus conclude that the adding together of the individual perturbations in quadrature gives a good approximation to the uncertainty calculated by the Monte Carlo method for significantly less computational burden.

6 Impacts on the present day atmosphere metrics

We show on Figure 2 the absolute percentage change in global annual mean O_3 burden, surface O_3, tropospheric average OH and CH_4 tropospheric lifetime from increasing each of the reaction rate constants in Table 1 in turn by their 1σ value. They are ordered by the magnitude of the perturbation and for clarity we only show the top 20, combining the remaining 40 in quadrature into the 'Other' category. The fractional change in tropospheric O_3 burden for all of the perturbations is given in Table 1. We show the results of combining all of these reactions in quadrature ('Total (sum)'), the result of combining the top 10 in quadrature ('Top 10') and the standard deviation from the 50 Monte-Carlo simulations ('Monte Carlo Top 10'). The relative closeness (~ 10%) of the value calculated from the 'Top 10' and the 'Monte Carlo Top 10' shows that the addition in quadrature approach provides a useful approximation to the Monte Carlo methodology with significantly less computational burden.

The top ten reactions contribute over 90% of the uncertainty for all metrics with the overall uncertainty for the annual mean tropospheric ozone burden, surface ozone and tropospheric OH concentrations, and tropospheric methane lifetime of calculated to be 11, 12, 17 and 17% respectively. These uncertainties can be compared to the inter-model spreads found from model inter-

Atmos. Chem. Phys. Discuss., doi:10.5194/acp-2017-12, 2017
Manuscript under review for journal Atmos. Chem. Phys.
Discussion started: 9 March 2017

Atmospheric Chemistry and Physics Discussions

comparison exercises. The multi-model standard deviation in the ozone burden, tropospheric OH concentration and troposphere methane lifetime were found to be 7%, 10% and 10% in the ACCMIP studies (Young et al., 2013; Voulgarakis et al., 2013). Thus we find that the chemical rate constant uncertainty is larger than the multi-model spread which is usually used to give some sense of our uncertainty in our understanding of a quantity. As the models used in these inter-comparisons typically use the same rate constants, this rate constant uncertainty is not included in the inter-model spread and so the inter-model spread should be considered the lower estimate for the uncertainty on parameters.

7 Spatial distribution of uncertainty

Figure 4 shows the spatial distribution of the total uncertainty in the annual mean O_3, OH and CO concentration, for the tropospheric column, the zonal mean, and at the surface from the 60 reactions. Similar plots for a large number of other model species are shown in Figures 5–10. There is a significant degree of in-homogeneity in these uncertainties which respond to a range of factors. The uncertainties in the rate constants are largest in the upper troposphere where the temperatures are coldest and thus furthest from the 298K base temperature used to calculate the uncertainties. However, these uncertainty can only manifest if chemistry is the large source or sink for a species in that region. O_3 uncertainties are relatively low in the upper troposphere as it has a large stratospheric source in this region which we have not perturbed (see Section 2). OH uncertainties on the other hand are high (30%) in the upper troposphere due to the low temperatures. Over continental regions the concentration of CO is not particularly uncertain as the emissions and transport control the concentration. However, over the ocean where emissions are small, the chemistry becomes more important and so uncertainty increases. Uncertainties in the CO are largest in the southern hemisphere where direct emission is low and chemical production from CH_4 and other hydrocarbons is significant. In general uncertainties are largest over remote regions far from recent emissions, especially if they are particularly cold or hot compared to room temperature. Thus surface OH values are more uncertain in the cold remote southern ocean than they are in the tropics. Surface O_3 values are uncertain in the warm tropics where intense sunlight and high water vapour concentrations leads to a large chemical flux through O_3.

Across the full set of simulated compounds (Figures 5–10) there are even larger uncertainties. For primary emitted hydrocarbons, large uncertainties occur in remote, photochemically active locations such as the topics where shorter lived hydrocarbons may be many OH lifetimes away from sources. Uncertainties in the OH concentrations thus multiply in these regions, leading to uncertainties of up to 60% for $\geq$C4 alkanes. Secondary products such as H_2O_2, CH_3OOH also show significant uncertainties of up to 56% in some locations.

NO_x concentrations close to emission sources are dominated by the emission and transport and so are not very sensitive to chemical uncertainty (Figure 7). However, away from these emissions uncertainties can build up. Uncertainty in the NO_x concentrations at the poles are up to a factor of 40%. Uncertainties in PAN concentrations 8 are in general high ($>$20%) in most locations ($\sim$ 50% over the remote ocean) reflecting the complexity of the chemistry involving uncertainties in both RO_x and NO_x concentrations. Uncertainties in nitric acid (the dominant NO_x sink) concentrations are smaller however ($\sim$5%) reflecting

Atmos. Chem. Phys. Discuss., doi:10.5194/acp-2017-12, 2017
Manuscript under review for journal Atmos. Chem. Phys.
Discussion started: 9 March 2017

Atmospheric Chemistry and Physics Discussions

the mass balance constraint of emissions of NO_x having to balance NO_y sinks. Large variability in nitric acid concentrations in the southern ocean reflects non-linearities in aerosol thermodynamics of HNO_3 / NO_3^- partitioning.

SO_2 concentrations show the largest uncertainties in the tropical upper troposphere where OH is also highly uncertain. However, SO_4^{2-} shows much smaller uncertainty, again reflecting mass conservation constraints. NH_4 concentrations show little sensitivity to the rate constants analysed. Overall this suggests that aerosol mass is not particularly sensitive to the gas phase chemistry examined here.

Overall, we see a complex pattern of uncertainty with geographically highly variable uncertainty.

8 Implications for model-measurement comparisons

Comparisons between the predictions made by models and observations underpin the assessment of model fidelity. Deviations between model and measurements are often used to diagnose model failings. Attributing these differences to uncertainties in the emissions is particularly popular (see for example Hartley and Prinn (1993); Huang et al. (2008)). Figure 11 shows observed monthly mean and standard deviations for CO, O_3, C_2H_6, C_3H_8, C_4H_{10} and NO_2 from the World Meteorological Organisation's Global Atmosphere Watch Cape Verde Atmospheric Observatory (Carpenter et al., 2011), overlaid with the base model simulation and the chemical uncertainty (1σ) calculated from the addition in quadrature of the 60 1σ simulations. We chose this location as it is far from recent emissions and so should show large uncertainties for primary emitted species.

Consistent with Figures 5–10 the uncertainty in the model calculation ranges from 5–30% depending upon the species. For some of the species (CO, O_3, C_2H_6, C_4H_{10}) much of the difference between the model and the measurements lie within the model 1σ uncertainty. For others such as C_3H_8 or NO_2 the differences are harder to explain and other processes (emissions, transport, unknown chemistry etc.) would need to be explored.

Figures 5–10 show significant changes in uncertainty with changes in the vertical due to increasing uncertainty with reducing temperature. Figure 13 shows a selection of ozonesonde observations from the World Ozone and Ultraviolet Data Centre (WOUDC) compared to equivalent modelled concentrations and uncertainties. Observations are derived from the surface into the middle troposphere as the temperature drops. The uncertainty thus maximises at around 10km. Above this much of the ozone in the model is produced in the stratosphere which is unperturbed in these simulations. Above this height the uncertainty in the ozone due to tropospheric chemistry uncertainty reduces.

These comparisons with observations highlight the complexity of attributing model failure to a particular cause. For some locations and for some species the chemical uncertainty can be large. For the same species, in a different location, the uncertainties may be much smaller. Inversion studies which attempt to attribute model failure to a single cause (for example uncertainties in emissions) need to have a detailed understanding of the magnitude and geographical distribution of the other model errors. We show here that they vary between different species, can be large and highly spatially varying. This should be considered when model inversion studies are undertaken.

Atmos. Chem. Phys. Discuss., doi:10.5194/acp-2017-12, 2017
Manuscript under review for journal Atmos. Chem. Phys.
Discussion started: 9 March 2017

Atmospheric Chemistry and Physics Discussions

9 Ozone radiative forcing

We repeat the 60 1σ simulations described above with pre-industrial (notionally the year 1850) emissions (see Section 2) to allow us to calculate an uncertainty in the radiative forcing of O_3. For each reaction we calculate the difference in the annual mean tropospheric column O_3 (Dobson Units) between the present day and pre-industrial with the rate constant increased to its 1σ value. Then using a linear relationship between change in O_3 column and radiative forcing (Stevenson et al., 2013; Young et al., 2013) of 42mW m^{-2} DU^{-1}, we calculate a radiative forcing associated with the uncertainty associated with each reaction. We estimate an overall uncertainty in the tropospheric O_3 radiative forcing in the same way as the other metrics, by adding them together in quadrature. In our base simulations we calculated the tropospheric O_3 radiative forcing to be 412 mWm^{-2} consistent with previous studies ($410 \pm 65 mWm^{-2}$) (Stevenson et al., 2013). Our estimate of the uncertainty in the O_3 radiative forcing from rate constant uncertainty is 56 mWm^{-2} (15%) with reaction specific detail shown in Figure 14. Again the same set of reactions contribute the largest share to the uncertainty in the radiative forcing as in the uncertainty in present day O_3 burden.

This uncertainty estimate of 15% can be compared to the 17% spread in the O_3 radiative forcing calculated between climate models in the recent ACCMIP (Young et al., 2013) inter-comparison (shown in Figure 14). This spread is usually used as the uncertainty in our understanding of O_3 radiative forcing. However, as all of these models use the same JPL or IUPAC recommended rate constants the inter-model spread does not include the rate constant uncertainty explored here. Given that the rate constant uncertainty is comparable to the inter-model spread, it should be included in future assessment of the uncertainty in O_3 radiative forcing. A naive addition in quadrature approach would suggest that the uncertainty on tropospheric O_3 radiative forcing should be increased by roughly 30% to account for this.

10 Discussion

We have shown that the uncertainty in the inorganic rate constants leads to significant (>10%) uncertainties in the concentration of policy relevant metrics of troposphere composition (O_3 burden, surface O_3, global mean OH, tropospheric CH_4 lifetime, O_3 radiative forcing) with significantly higher uncertainty in other compounds. This uncertainty may have implications for climate policy through an underestimate of the uncertainty on O_3 radiative forcing or significant uncertainties on the CH_4 lifetime. This also has implication for how model-measurement disagreements are interpreted. Similar conclusions have been found for regional air quality focussed models (Yang et al., 2000).

The simulation performed here likely provide a lower limit to the chemical uncertainty. We do not explore the impact in uncertainties in organic chemistry (beyond that from the initiation of hydrocarbon oxidation) or in organic mechanisms; we do not included tropospheric bromine, iodine, chlorine chemistry in our analysis or heterogeneous parameters. We have neither investigated the impact of rate constant uncertainty on the composition of the stratosphere or mesosphere, or how this may propagate through to the troposphere. There are also uncertainties in the Henry's Law constants used for wet and dry parameterisations etc. It seems likely therefore that the true chemical uncertainty in the composition of the atmosphere is significantly higher than that found here.

Atmos. Chem. Phys. Discuss., doi:10.5194/acp-2017-12, 2017
Manuscript under review for journal Atmos. Chem. Phys.
Discussion started: 9 March 2017

Atmospheric Chemistry and Physics Discussions

Although it may be challenging, reducing these uncertainties would provide significant benefits. Targeting the top 10 reactions identified here (Figure 2 (a)) would significantly reduce the overall chemical uncertainties. Despite the fact that these reactions may appear rather un-interesting to some, they provide the basis for determining the composition of the atmosphere. Given the difficulties in reducing the uncertainties in other areas of the climate system (we will never know the pre-industrial emissions well etc.) a redoubled effort to reduce rate constant uncertainty appears to be a relatively straightforward methodology to improve our understanding of atmospheric composition.

Acknowledgements. Ben Newsome was supported by a NERC Studentship (NE/L501761/1). This work was supported by the NERC funded BACCHUS project (NE/L01291X/1). The Cape Verde Atmospheric Observatory is supported by the NERC funded ORC3 project (NE/K004980/1) and by the National Centre for Atmospheric Science. GEOS-Chem (www.geos-chem.org) is a community effort and we wish to thank all involved in the development of the model. We would also thank all the JPL and IUPAC panels for their efforts in compiling atmospheric rate constants.

References

Atkinson, R., Baulch, D. L., Cox, R. A., Crowley, J. N., Hampson, R. F., Hynes, R. G., Jenkin, M. E., Rossi, M. J., and Troe, J.: Evaluated kinetic and photochemical data for atmospheric chemistry: Volume I - gas phase reactions of O_x, HO_x, NO_x and SO_x species, Atmos. Chem. Phys., 4, 1461–1738, doi:10.5194/acp-4-1461-2004, http://www.atmos-chem-phys.net/4/1461/2004/, 2004.

Bey, I., Jacob, D. J., Yantosca, R. M., Logan, J. A., Field, B. D., Fiore, A. M., Li, Q., Liu, H. Y., Mickley, L. J., and Schultz, M. G.: Global modeling of tropospheric chemistry with assimilated meteorology: Model description and evaluation, J. Geophys. Res. Atmos., 106, 23 073–23 095, doi:10.1029/2001JD000807, http://dx.doi.org/10.1029/2001JD000807, 2001.

Carpenter, L. J., Fleming, Z. L., Read, K. A., Lee, J. D., Moller, S. J., Hopkins, J. R., Purvis, R. M., Lewis, A. C., Müller, K., Heinold, B., Herrmann, H., Fomba, K. W., van Pinxteren, D., Müller, C., Tegen, I., Wiedensohler, A., Müller, T., Niedermeier, N., Achterberg, E. P., Patey, M. D., Kozlova, E. A., Heimann, M., Heard, D. E., Plane, J. M. C., Mahajan, A., Oetjen, H., Ingham, T., Stone, D., Whalley, L. K., Evans, M. J., Pilling, M. J., Leigh, R. J., Monks, P. S., Karunaharan, A., Vaughan, S., Arnold, S. R., Tschritter, J., Pöhler, D., Frieß, U., Holla, R., Mendes, L. M., Lopez, H., Faria, B., Manning, A. J., and Wallace, D. W. R.: Seasonal characteristics of tropical marine boundary layer air measured at the Cape Verde Atmospheric Observatory, Journal of Atmospheric Chemistry, 67, 87–140, doi:10.1007/s10874-011-9206-1, http://dx.doi.org/10.1007/s10874-011-9206-1, 2011.

Dockery, D. W., Pope, C. A., Xu, X., Spengler, J. D., Ware, J. H., Fay, M. E., Ferris, B. G. J., and Speizer, F. E.: An Association between Air Pollution and Mortality in Six U.S. Cities, N. Engl. J. Med., 329, 1753–1759, doi:10.1056/NEJM199312093292401, http://dx.doi.org/10.1056/NEJM199312093292401, 1993.

Goldstein, A. H. and Galbally, I. E.: Known and Unexplored Organic Constituents in the Earth's Atmosphere, Environmental Science & Technology, 41, 1514–1521, doi:10.1021/es072476p, http://dx.doi.org/10.1021/es072476p, 2007.

Hartley, D. and Prinn, R.: Feasibility of determining surface emissions of trace gases using an inverse method in a three-dimensional chemical transport model, J. Geophys. Res. Atmos., 98, 5183–5197, doi:10.1029/92JD02594, http://dx.doi.org/10.1029/92JD02594, 1993.

Huang, J., Golombek, A., Prinn, R., Weiss, R., Fraser, P., Simmonds, P., Dlugokencky, E. J., Hall, B., Elkins, J., Steele, P., Langenfelds, R., Krummel, P., Dutton, G., and Porter, L.: Estimation of regional emissions of nitrous oxide from 1997 to 2005 using multinetwork measurements, a chemical transport model, and an inverse method, J. Geophys. Res. Atmos., 113, doi:10.1029/2007JD009381, http://dx.doi.org/10.1029/2007JD009381, 2008.

Hudman, R. C., Moore, N. E., Mebust, A. K., Martin, R. V., Russell, A. R., Valin, L. C., and Cohen, R. C.: Steps towards a mechanistic model of global soil nitric oxide emissions: implementation and space based-constraints, Atmos. Chem. Phys., 12, 7779–7795, doi:10.5194/acp-12-7779-2012, http://www.atmos-chem-phys.net/12/7779/2012/, 2012.

Jacobson, M. Z. and Turco, R. P.: SMVGEAR: A sparse-matrix, vectorized Gear code for atmospheric models, Atmospheric Environment, 28, 273–284, 1994.

Lin, X., Trainer, M., and Liu, S. C.: On the nonlinearity of the tropospheric ozone production, J. Geophys. Res. Atmos., 93, 15 879–15 888, doi:10.1029/JD093iD12p15879, http://dx.doi.org/10.1029/JD093iD12p15879, 1988.

McLinden, C., Olsen, S., Hannegan, B., Wild, O., Prather, M., and Sundet, J.: Stratospheric ozone in 3-D models: A simple chemistry and the cross-tropopause flux, J. Geophys. Res., 105, 2000.

Murray, L. T., Jacob, D. J., Logan, J. A., Hudman, R. C., and Koshak, W. J.: Optimized regional and interannual variability of lightning in a global chemical transport model constrained by LIS/OTD satellite data, J. Geophys. Res. Atmos., 117, doi:10.1029/2012JD017934, http://dx.doi.org/10.1029/2012JD017934, 2012.

Park, R. J., Jacob, D. J., Chin, M., and Martin, R. V.: Sources of carbonaceous aerosols over the United States and implications for natural visibility, J. Geophys. Res. Atmos., 108, doi:10.1029/2002JD003190, http://dx.doi.org/10.1029/2002JD003190, 2003.

Parrella, J. P., Jacob, D. J., Liang, Q., Zhang, Y., Mickley, L. J., Miller, B., Evans, M. J., Yang, X., Pyle, J. A., Theys, N., and Van Roozendael, M.: Tropospheric bromine chemistry: implications for present and pre-industrial ozone and mercury, Atmos. Chem. Phys., 12, 6723–6740, doi:10.5194/acp-12-6723-2012, http://www.atmos-chem-phys.net/12/6723/2012/, 2012.

Sander, S. P., Abbatt, J., Burkholder, J. R. B. J. B., Friedl, R. R., Golden, D. M., Huie, R. E., Kolb, C. E., Kurylo, M. J., Moortgat, G., Orkin, V. L., and Wine, P. H.: Chemical Kinetics and Photochemical Data for Use in Atmospheric Studies, Evaluation No. 17, Jet Propulsion Laboratory, http://jpldataeval.jpl.nasa.gov/, 2011.

Sherwen, T., Evans, M. J., Carpenter, L. J., Andrews, S. J., Lidster, R. T., Dix, B., Koenig, T. K., Sinreich, R., Ortega, I., Volkamer, R., Saiz-Lopez, A., Prados-Roman, C., Mahajan, A. S., and Ordóñez, C.: Iodine's impact on tropospheric oxidants: a global model study in GEOS-Chem, Atmos. Chem. Phys., 16, 1161–1186, doi:10.5194/acp-16-1161-2016, http://www.atmos-chem-phys.net/16/1161/2016/, 2016.

Sindelarova, K., Granier, C., Bouarar, I., Guenther, A., Tilmes, S., Stavrakou, T., Müller, J.-F., Kuhn, U., Stefani, P., and Knorr, W.: Global data set of biogenic VOC emissions calculated by the MEGAN model over the last 30 years, Atmos. Chem. Phys., 14, 9317–9341, doi:10.5194/acp-14-9317-2014, http://www.atmos-chem-phys.net/14/9317/2014/, 2014.

Sofen, E. D., Alexander, B., and Kunasek, S. A.: The impact of anthropogenic emissions on atmospheric sulfate production pathways, oxidants, and ice core, Atmos. Chem. Phys., 11, 3565–3578, doi:10.5194/acp-11-3565-2011, http://www.atmos-chem-phys.net/11/3565/2011/, 2011.

Sofen, E. D., Bowdalo, D., Evans, M. J., Apadula, F., Bonasoni, P., Cupeiro, M., Ellul, R., Galbally, I. E., Girgzdiene, R., Luppo, S., Mimouni, M., Nahas, A. C., Saliba, M., and Tørseth, K.: Gridded global surface ozone metrics for atmospheric chemistry model evaluation, Earth System Science Data, 8, 41–59, doi:10.5194/essd-8-41-2016, http://www.earth-syst-sci-data.net/8/41/2016/, 2016.

Stevenson, D. S., Young, P. J., Naik, V., Lamarque, J.-F., Shindell, D. T., Voulgarakis, A., Skeie, R. B., Dalsoren, S. B., Myhre, G., Berntsen, T. K., Folberth, G. A., Rumbold, S. T., Collins, W. J., MacKenzie, I. A., Doherty, R. M., Zeng, G., van Noije, T. P. C., Strunk, A., Bergmann, D., Cameron-Smith, P., Plummer, D. A., Strode, S. A., Horowitz, L., Lee, Y. H., Szopa, S., Sudo, K., Nagashima, T., Josse, B., Cionni, I., Righi, M., Eyring, V., Conley, A., Bowman, K. W., Wild, O., and Archibald, A.: Tropospheric ozone changes, radiative forcing and attribution to emissions in the Atmospheric Chemistry and Climate Model Intercomparison Project (ACCMIP), Atmos. Chem. Phys., 13, 3063–3085, doi:10.5194/acp-13-3063-2013, http://www.atmos-chem-phys.net/13/3063/2013/, 2013.

Stocker, T. F.: Climate change 2013: the physical science basis: Working Group I contribution to the Fifth assessment report of the Intergovernmental Panel on Climate Change, Cambridge University Press, 2014.

van der Werf, G. R., Randerson, J. T., Giglio, L., Collatz, G. J., Mu, M., Kasibhatla, P. S., Morton, D. C., DeFries, R. S., Jin, Y., and van Leeuwen, T. T.: Global fire emissions and the contribution of deforestation, savanna, forest, agricultural, and peat fires (1997â€“2009), Atmos. Chem. Phys., 10, 11 707–11 735, doi:10.5194/acp-10-11707-2010, http://www.atmos-chem-phys.net/10/11707/2010/, 2010.

Voulgarakis, A., Naik, V., Lamarque, J.-F., Shindell, D. T., Young, P. J., Prather, M. J., Wild, O., Field, R. D., Bergmann, D., Cameron-Smith, P., Cionni, I., Collins, W. J., Dalsøren, S. B., Doherty, R. M., Eyring, V., Faluvegi, G., Folberth, G. A., Horowitz, L. W., Josse, B., MacKenzie, I. A., Nagashima, T., Plummer, D. A., Righi, M., Rumbold, S. T., Stevenson, D. S., Strode, S. A., Sudo, K., Szopa, S., and Zeng, G.: Analysis of present day and future OH and methane lifetime in the ACCMIP simulations, Atmos. Chem. Phys., 13, 2563–2587, doi:10.5194/acp-13-2563-2013, http://www.atmos-chem-phys.net/13/2563/2013/, 2013.

WOUDC: WOUDC Ozone Monitoring Community, World Meteorological Organization-Global Atmosphere Watch Program (WMO-GAW), doi:10.14287/10000001, http://www.woudc.org.

Yang, Y.-J., Wilkinson, J. G., Talat Odman, M., and Russell, A. G.: Air Pollution Modeling and Its Application XIII, chap. Ozone Sensitivity and Uncertainty Analysis Using DDM-3D in a Photochemical Air Quality Model, pp. 183–194, Springer US, Boston, MA, doi:10.1007/978-1-4615-4153-0_19, http://dx.doi.org/10.1007/978-1-4615-4153-0_19, 2000.

Young, P. J., Archibald, A. T., Bowman, K. W., Lamarque, J.-F., Naik, V., Stevenson, D. S., Tilmes, S., Voulgarakis, A., Wild, O., Bergmann, D., Cameron-Smith, P., Cionni, I., Collins, W. J., Dalsøren, S. B., Doherty, R. M., Eyring, V., Faluvegi, G., Horowitz, L. W., Josse, B., Lee, Y. H., MacKenzie, I. A., Nagashima, T., Plummer, D. A., Righi, M., Rumbold, S. T., Skeie, R. B., Shindell, D. T., Strode, S. A., Sudo, K., Szopa, S., and Zeng, G.: Pre-industrial to end 21st century projections of tropospheric ozone from the Atmospheric Chemistry and Climate Model Intercomparison Project (ACCMIP), Atmos. Chem. Phys., 13, 2063–2090, doi:10.5194/acp-13-2063-2013, http://www.atmos-chem-phys.net/13/2063/2013/, 2013.

Atmos. Chem. Phys. Discuss., doi:10.5194/acp-2017-12, 2017
Manuscript under review for journal Atmos. Chem. Phys.
Discussion started: 9 March 2017

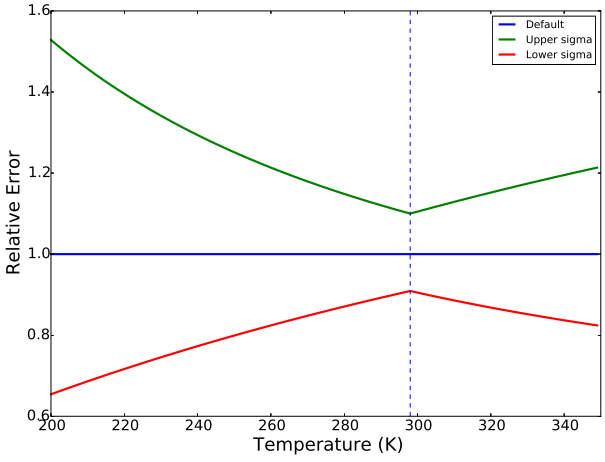

Figure 1. Example of the uncertainty on a reaction rate constant. The relative uncertainty of the reaction O_3 + NO is plotted as a function of temperature. The lowest uncertainty is at room temperature (298K) with exponentially increasing uncertainties occurring as we diverge to higher and lower temperatures.

Atmos. Chem. Phys. Discuss., doi:10.5194/acp-2017-12, 2017
Manuscript under review for journal Atmos. Chem. Phys.
Discussion started: 9 March 2017

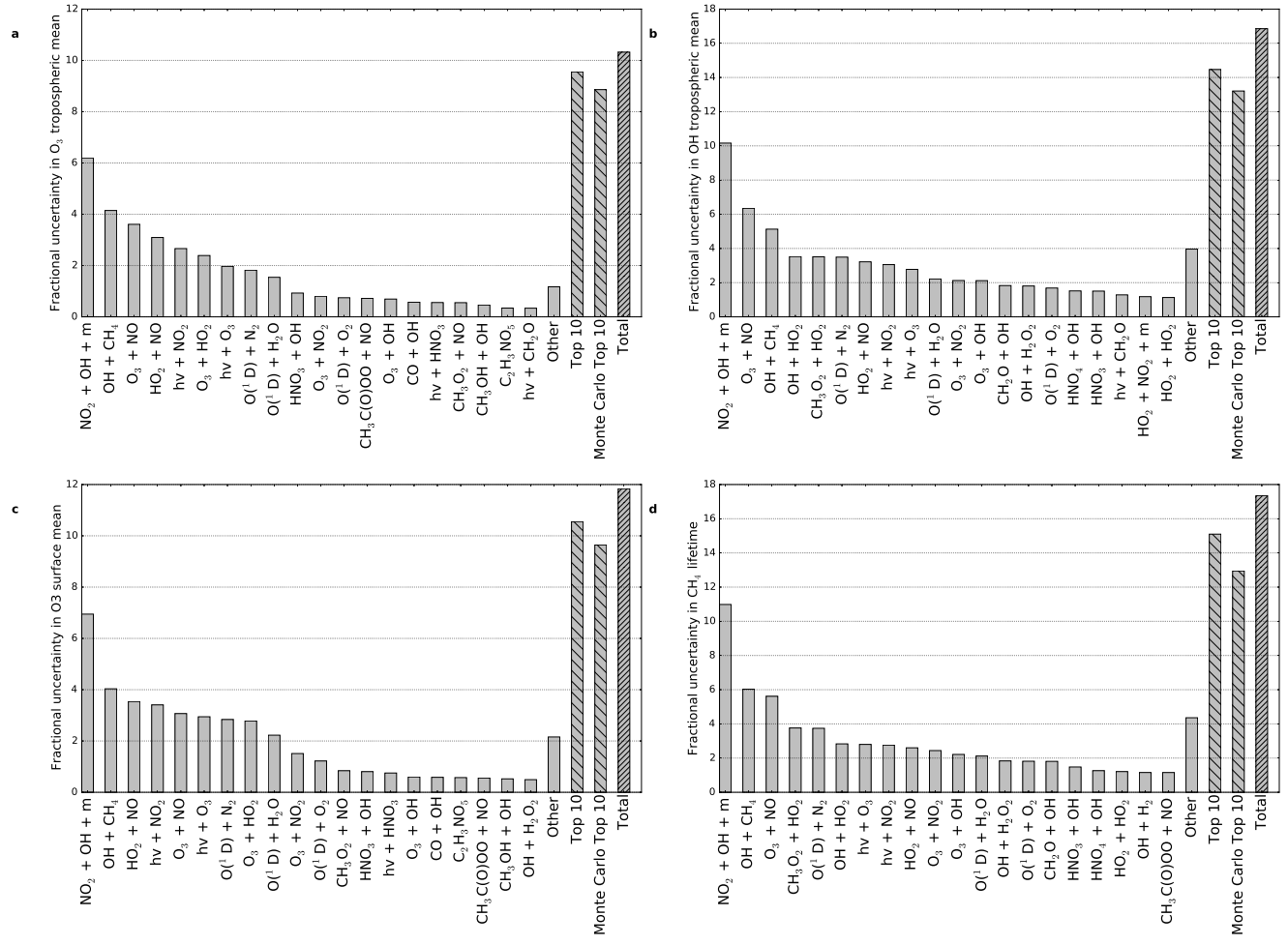

Figure 2. Uncertainties in all metrics. Fractional uncertainties of **a** O_3 tropospheric burden, **b** OH tropospheric burden, **c** O_3 surface concentration and **d** CH_4 lifetime. Each bar labelled with a reaction represents a run with a 1σ increase in the rate constant. 'Other' represents the addition in quadrature of the reactions that were not the top 20 most influential. 'Total (Top 10)' represents the addition in quadrature of the 10 most important reactions, and 'Monte Carlo Top 10' represents the standard deviation of the Monte Carlo ensemble. 'Total' represents the addition in quadrature of all the simulations.

Atmos. Chem. Phys. Discuss., doi:10.5194/acp-2017-12, 2017
Manuscript under review for journal Atmos. Chem. Phys.
Discussion started: 9 March 2017

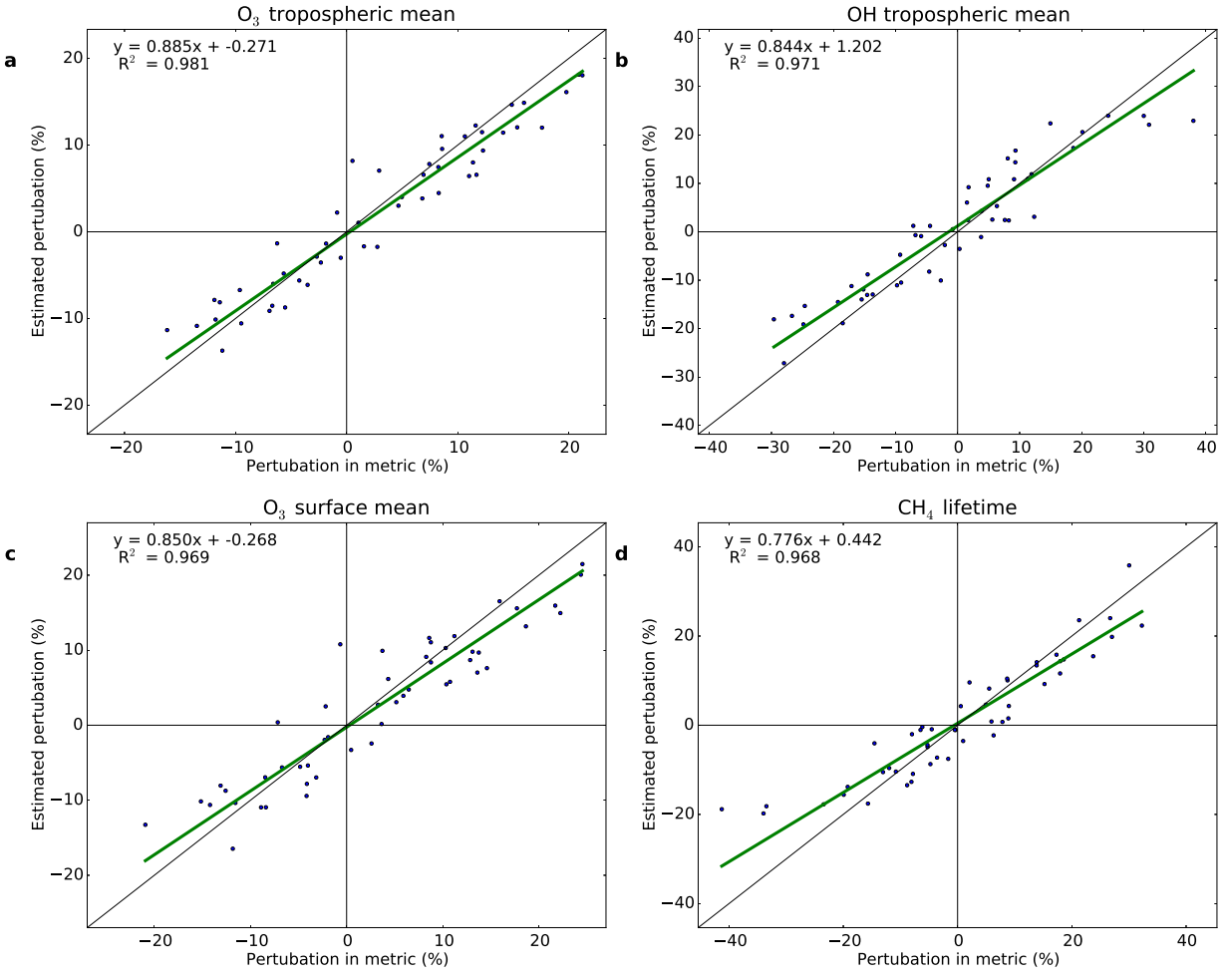

Figure 3. Monte Carlo simulations to understand the models linearity. The X axis values shows the percentage change in the metric value of an ensemble member compared to the simulation with no perturbations. The Y axis values show the expected percentage change of the metric based on a linear addition of the individual 1 sigma perturbation experiments weighted by the Monte Carlo perturbation values. Metrics investigates are **a** O_3 tropospheric burden, **b** O_3 mean surface concentration, **c** OH tropospheric burden and **d** CH_4 lifetime. We show the result of 50 Monte Carlo simulations. Each simulation perturbs 10 of the most important reactions (* reactions in SI Table 1) 1σ by normally distributed random numbers.

Atmos. Chem. Phys. Discuss., doi:10.5194/acp-2017-12, 2017
Manuscript under review for journal Atmos. Chem. Phys.
Discussion started: 9 March 2017

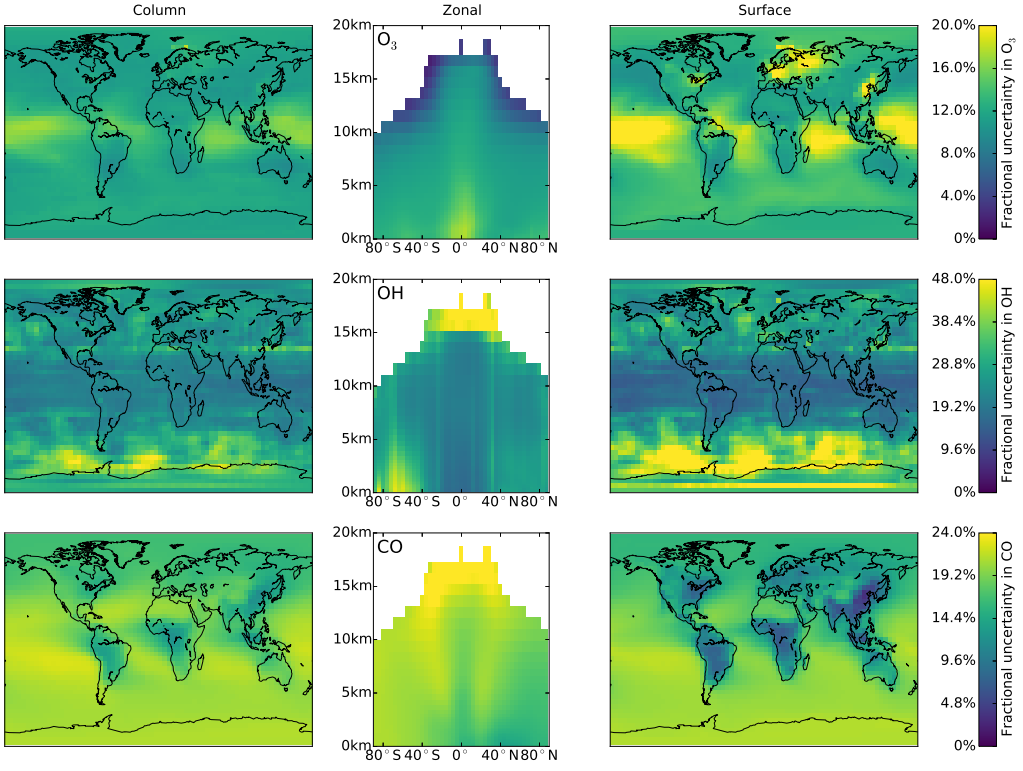

Figure 4. Spatial distribution of uncertainties. Fractional uncertainties calculated for O_3, OH and CO concentrations for the tropospheric column (left), the zonal mean (centre) and the surface (right) from adding together the individual reaction uncertainties from the 60 reactions studied in quadrature

Atmos. Chem. Phys. Discuss., doi:10.5194/acp-2017-12, 2017
Manuscript under review for journal Atmos. Chem. Phys.
Discussion started: 9 March 2017

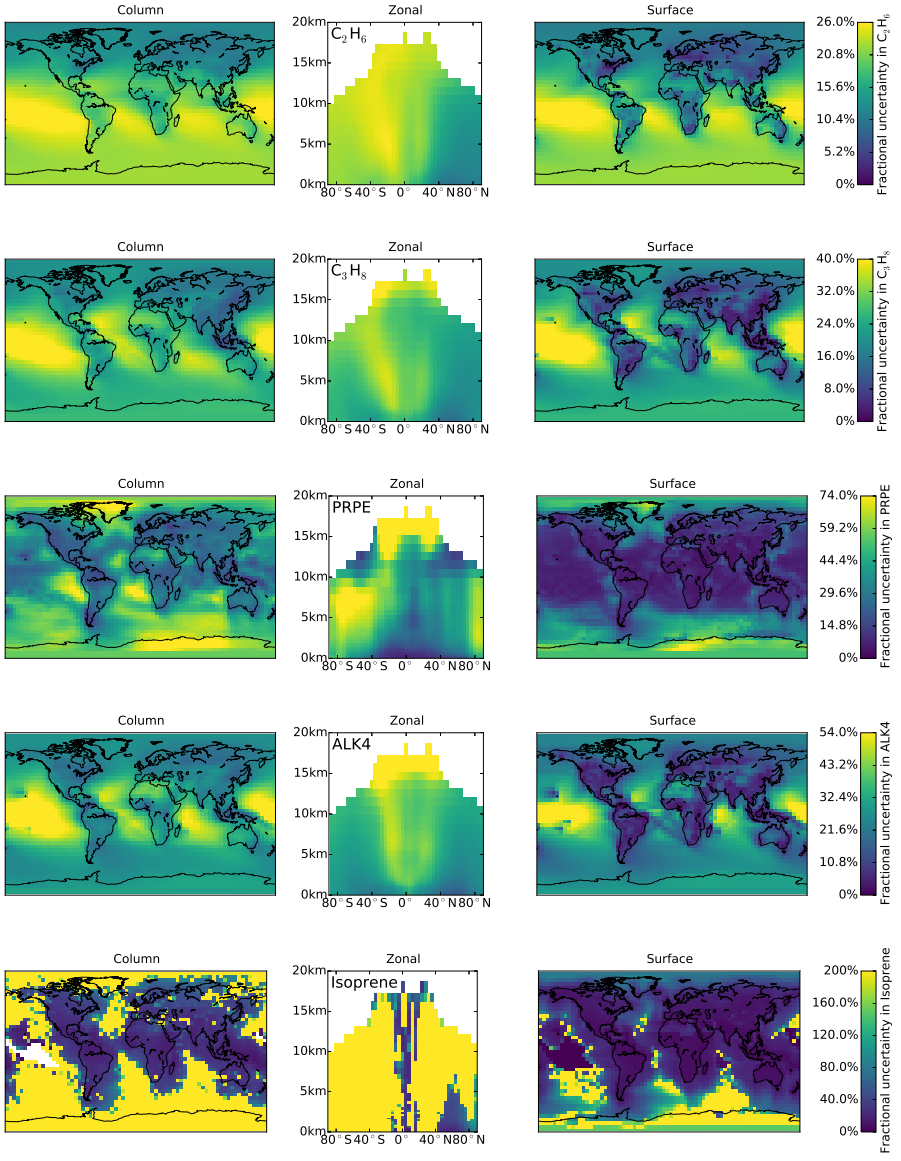

Figure 5. Primary VOCs. Total 1σ uncertainty in the concentrations of C_2H_6, C_3H_8, PRPE ($\geq$ C3 Alkenes), ALK4 ($\geq$ C4 Alkanes) and ISOP (Isoprene) from the addition in quadrature of the individual reaction uncertainties. Column covers the tropospheric column.

Atmos. Chem. Phys. Discuss., doi:10.5194/acp-2017-12, 2017
Manuscript under review for journal Atmos. Chem. Phys.
Discussion started: 9 March 2017

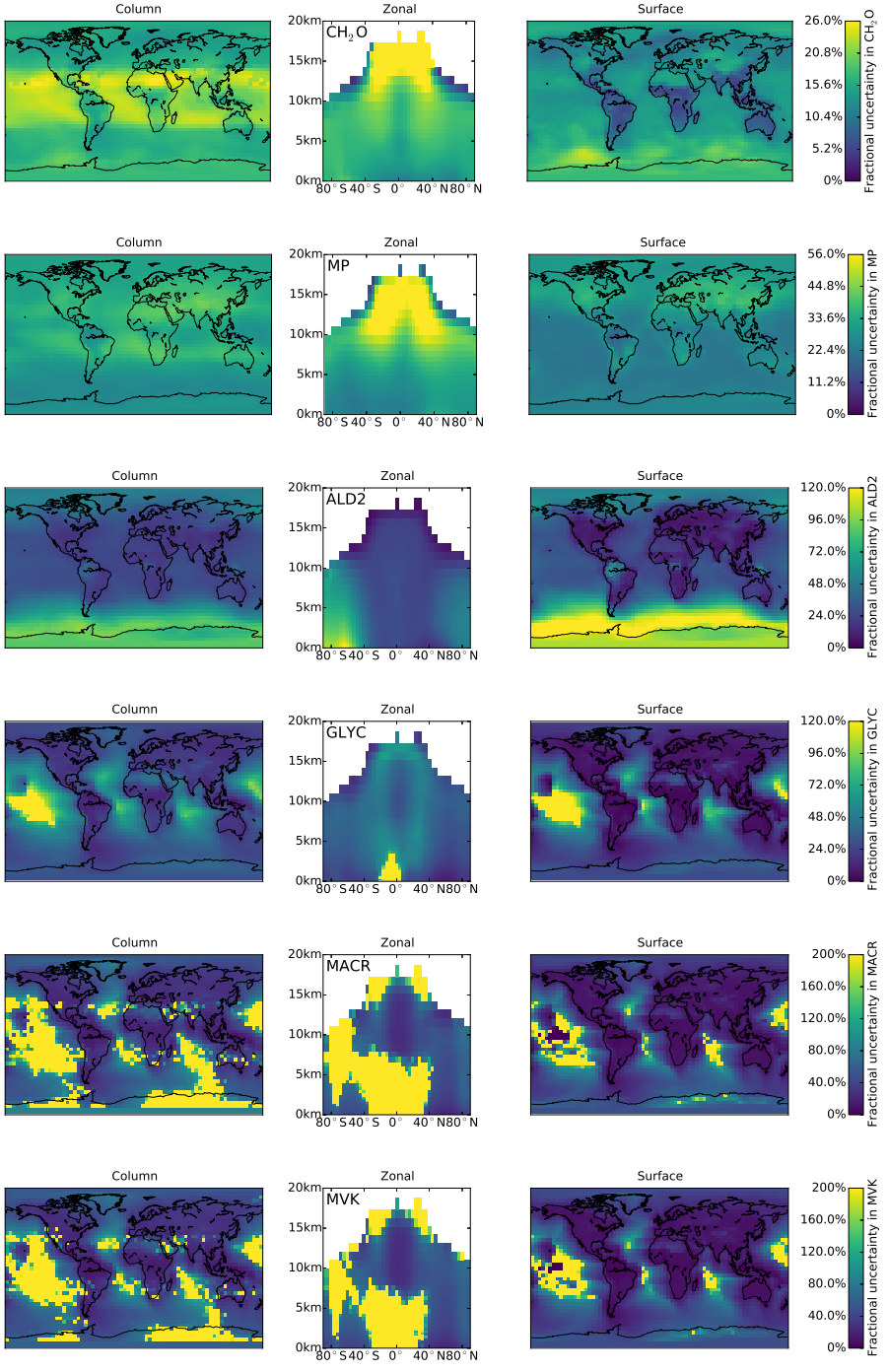

Figure 6. Other Organics. Total 1σ uncertainty in the concentrations of CH_2O, MP (Methyl Hydro Peroxide), ALD2 (Acetaldehyde), GLYC (Glycoaldehyde), MACR (Methacrolein) and MKV (Methyl Vinyl Ketone) from the addition in quadrature of the individual reaction uncertainties. Column covers the tropospheric column.

Atmos. Chem. Phys. Discuss., doi:10.5194/acp-2017-12, 2017
Manuscript under review for journal Atmos. Chem. Phys.
Discussion started: 9 March 2017

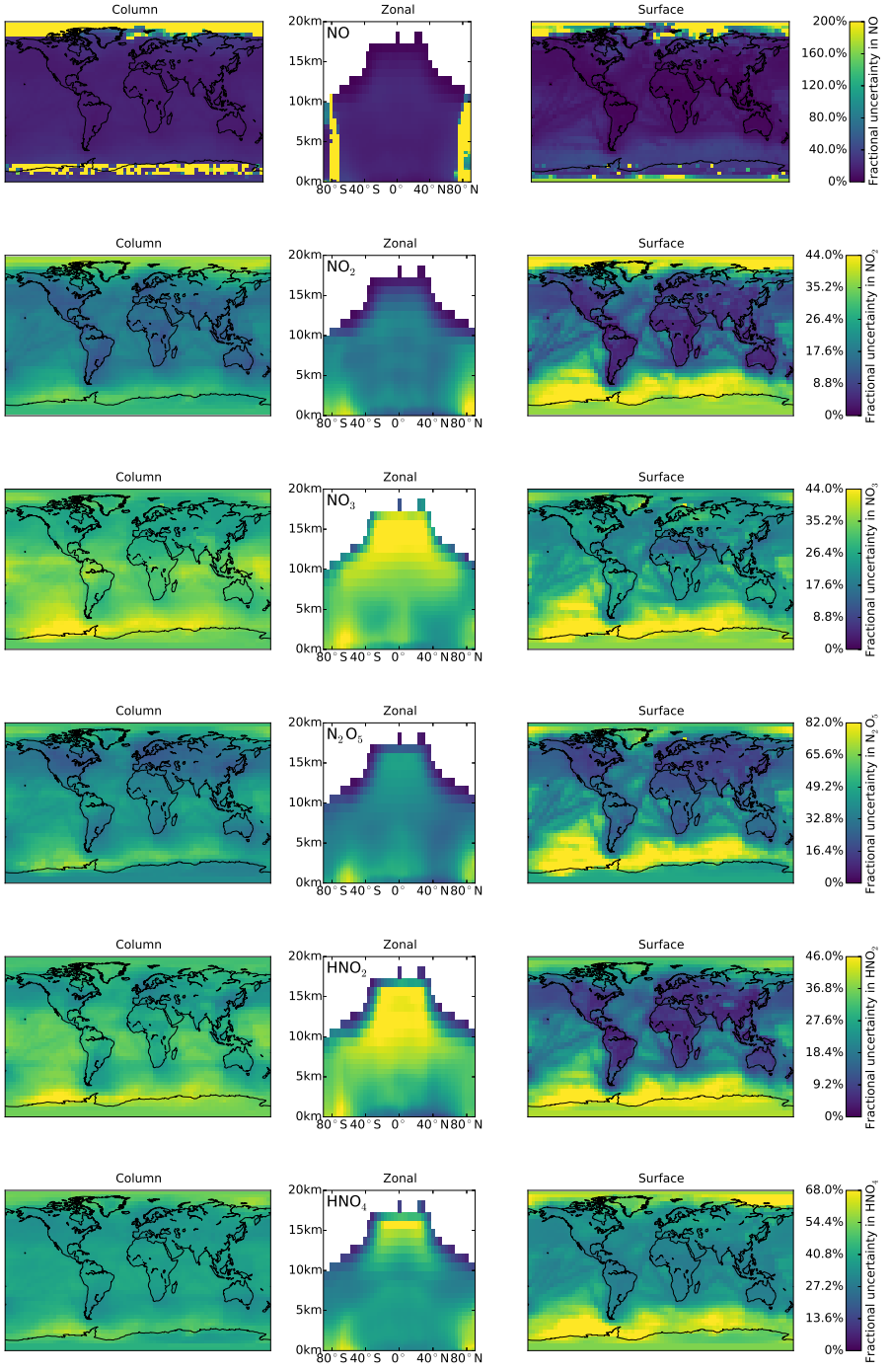

Figure 7. NO_x. Total 1σ uncertainty in the concentrations of NO, NO_2, NO_3, N_2O_5, HNO_2 and HNO_4 from the addition in quadrature of the individual reaction uncertainties. Column covers the tropospheric column.

Atmos. Chem. Phys. Discuss., doi:10.5194/acp-2017-12, 2017
Manuscript under review for journal Atmos. Chem. Phys.
Discussion started: 9 March 2017

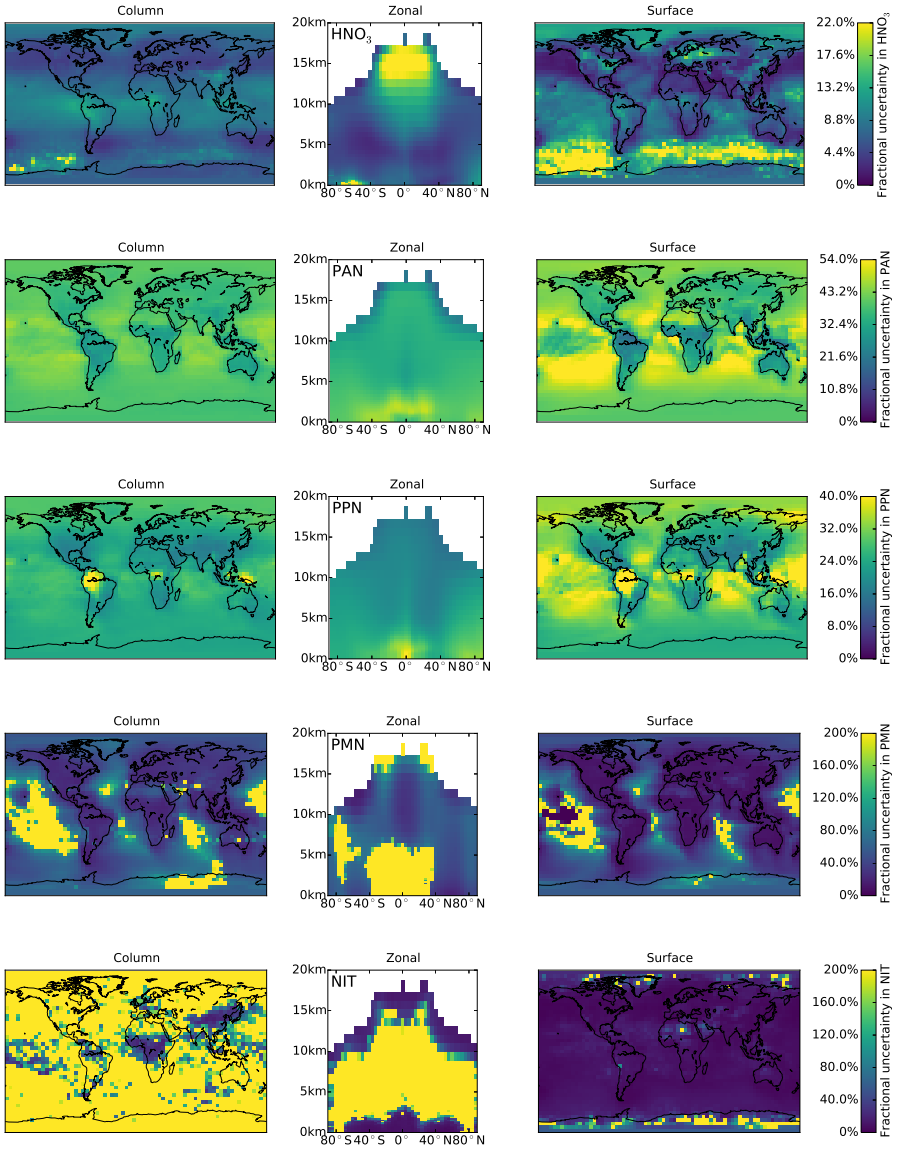

Figure 8. NO_y. Total 1σ uncertainty in the concentrations of HNO_3, PAN (Peroxyacetyl Nitrate), PPN (Peroxymethacroyl Nitrate), PMN (Peroxymethacroyl Nitrate) and NIT (Inorganic nitrates) from the addition in quadrature of the individual reaction uncertainties. Column covers the tropospheric column.

Atmos. Chem. Phys. Discuss., doi:10.5194/acp-2017-12, 2017
Manuscript under review for journal Atmos. Chem. Phys.
Discussion started: 9 March 2017

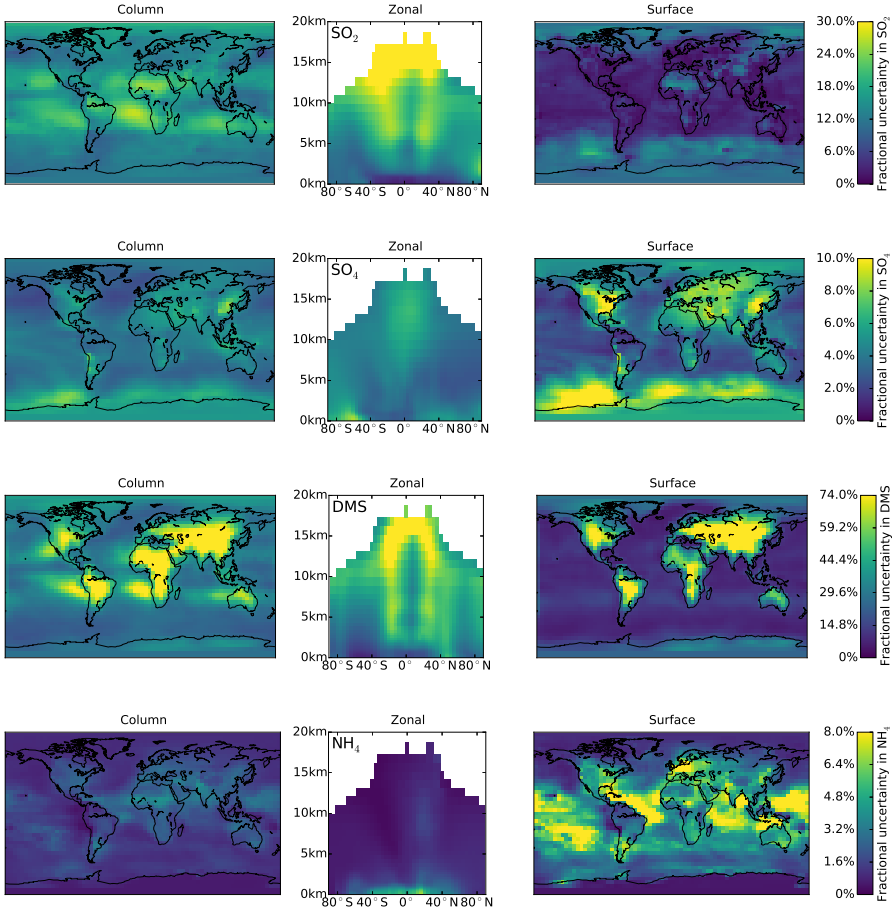

Figure 9. Sulfur and Aerosols. Total 1σ uncertainty in the concentrations of SO_2, SO_4, DMS (Dimethyl Sulfide) and NH_4 from the addition in quadrature of the individual reaction uncertainties. Column covers the tropospheric column.

Atmos. Chem. Phys. Discuss., doi:10.5194/acp-2017-12, 2017
Manuscript under review for journal Atmos. Chem. Phys.
Discussion started: 9 March 2017

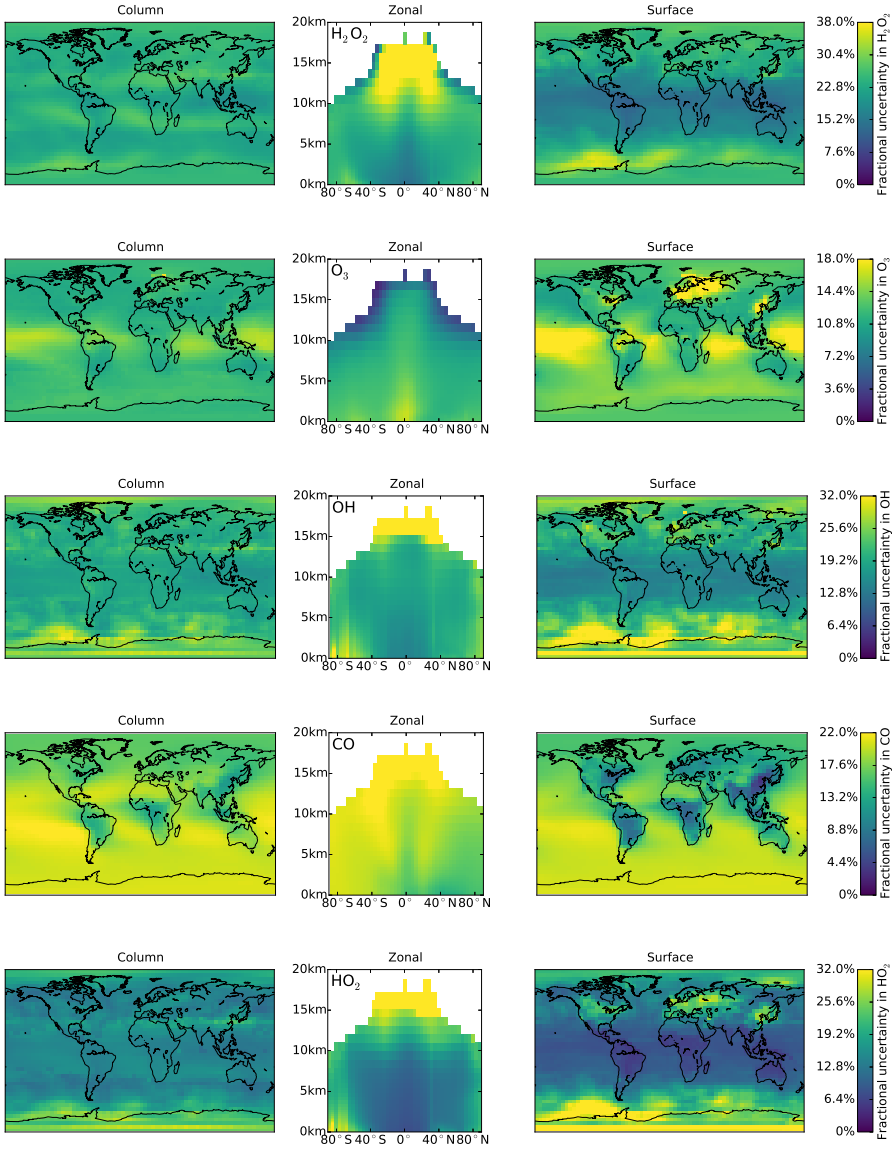

Figure 10. Inorganics. Total 1σ uncertainty in the concentrations of H_2O_2, O_3, OH, CO and HO_2 from the addition in quadrature of the individual reaction uncertainties. Column covers the tropospheric column.

Atmos. Chem. Phys. Discuss., doi:10.5194/acp-2017-12, 2017
Manuscript under review for journal Atmos. Chem. Phys.
Discussion started: 9 March 2017

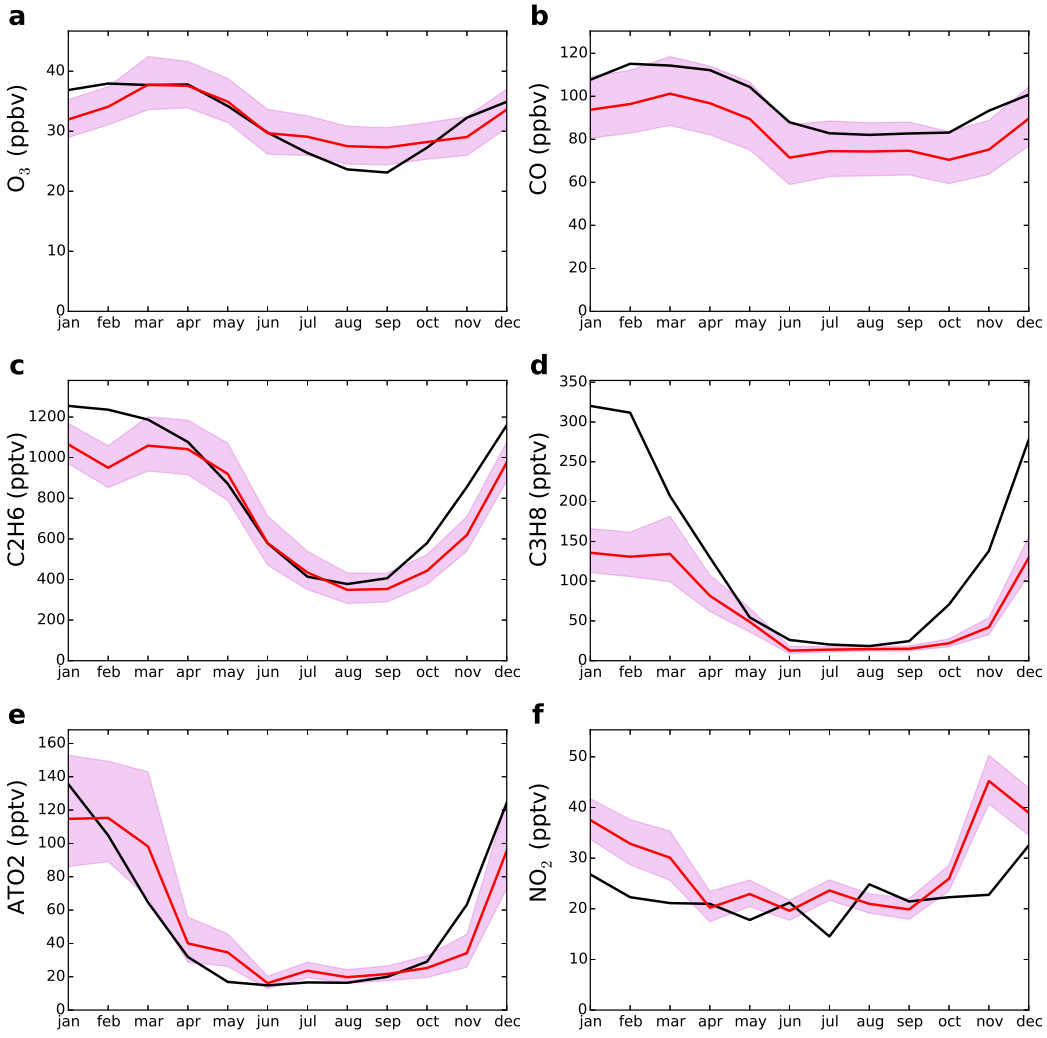

Figure 11. Impact on model / measurement comparisons. Modelled (red) and measured (black) annual cycle in monthly mean O_3, CO, C_2H_6, C_3H_8, ALK4 ($\geq$ C4 Alkanes) and NO_2 mixing ratios at Cape Verde (Carpenter et al., 2011). Shaded area represents the 1σ uncertainty from the 60 reactions added together in quadrature.

Atmos. Chem. Phys. Discuss., doi:10.5194/acp-2017-12, 2017
Manuscript under review for journal Atmos. Chem. Phys.
Discussion started: 9 March 2017

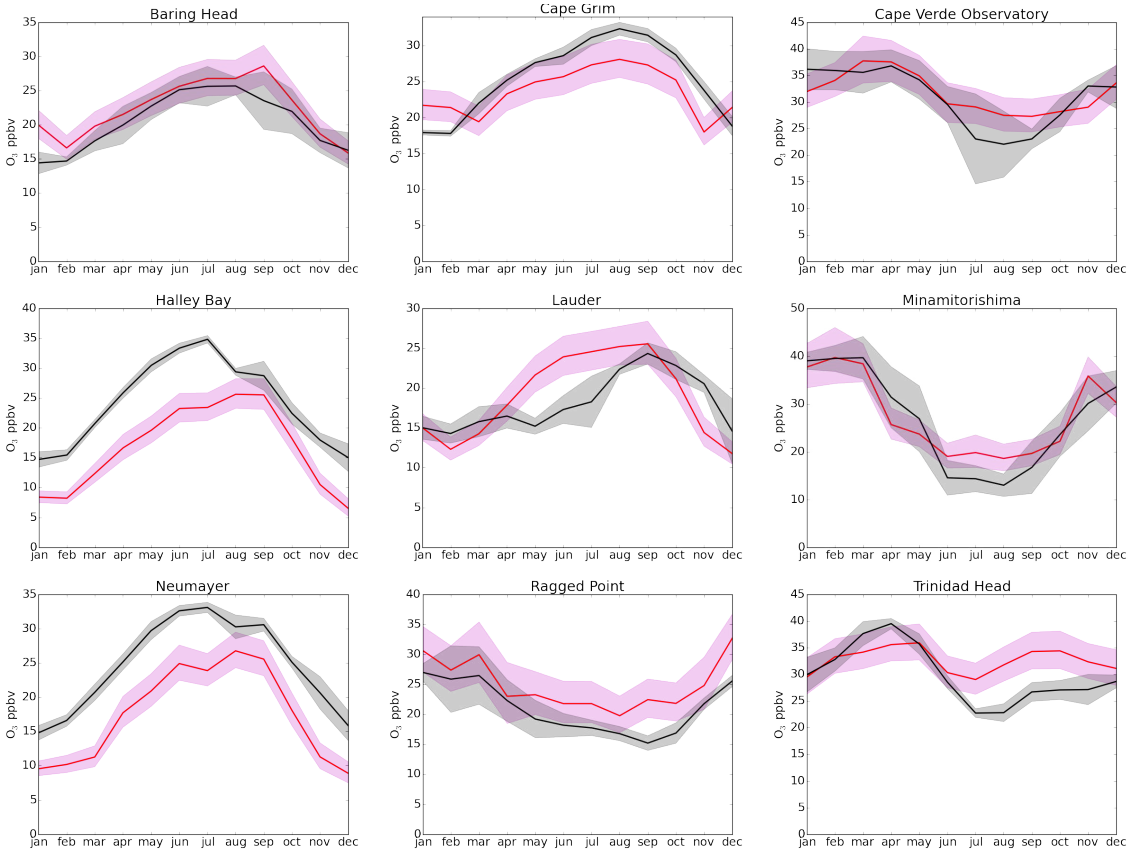

Figure 12. Ozone site comparison Modelled (red) and measured (black) concentrations of ozone at a range of sites. The pink shaded area shows the 1sigma uncertainty from the chemical kinetics. The error bars represent the 1sigma uncertainty of these observations. Monthly mean observational data obtained from (Sofen and Evans, 2015) (Sofen et al., 2016), using multiple years between 2004 and 2010 to create more complete datasets.

Atmos. Chem. Phys. Discuss., doi:10.5194/acp-2017-12, 2017
Manuscript under review for journal Atmos. Chem. Phys.
Discussion started: 9 March 2017

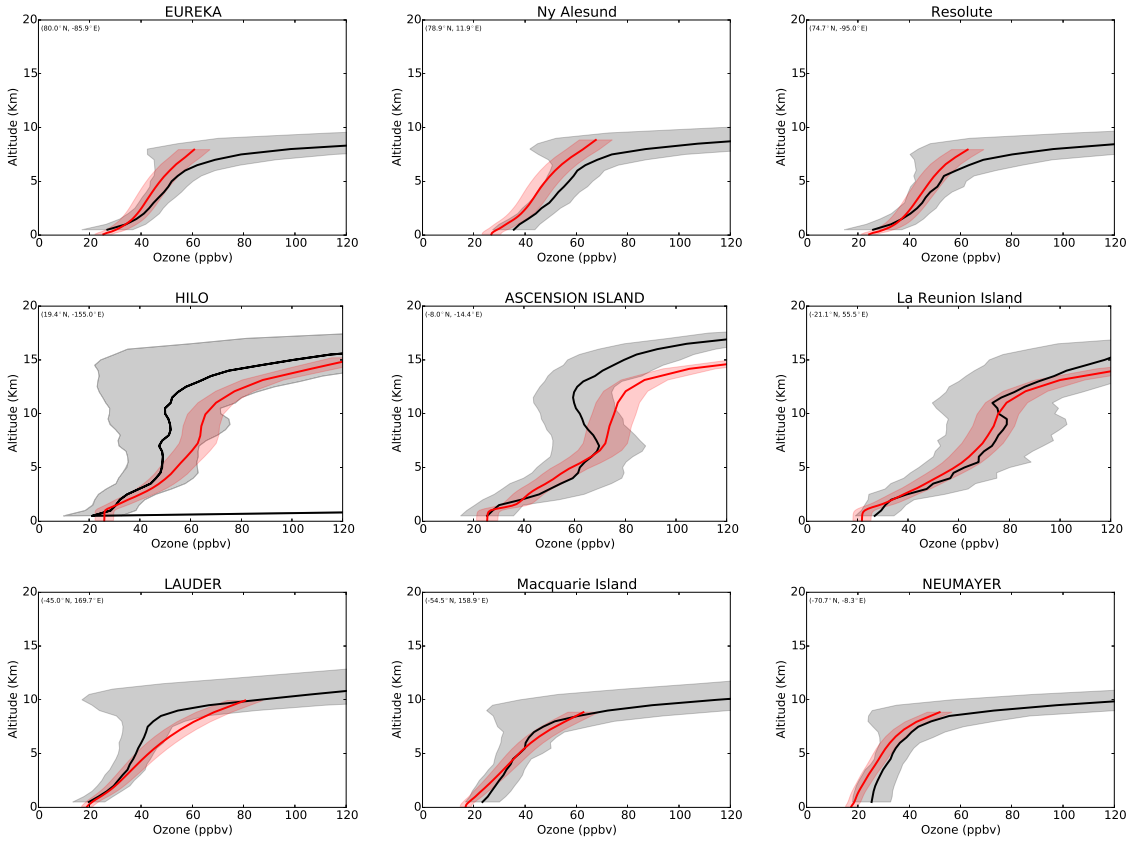

Figure 13. Ozonesonde Comparisons between the variability of annual ozonesonde measurements and model data with uncertainties. The black line shows the annual mean observation data and the shaded gray shows the range of data. The red line shows the model data and the pink shaded line shows the chemical 1sigma uncertainty. Observations are obtained from WOUDC (2014)(WOUDC).

Atmos. Chem. Phys. Discuss., doi:10.5194/acp-2017-12, 2017
Manuscript under review for journal Atmos. Chem. Phys.
Discussion started: 9 March 2017

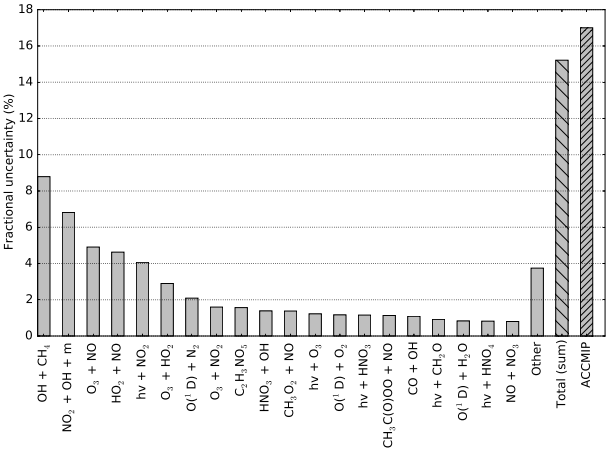

Figure 14. Uncertainties in O_3 radiative forcing. Absolute fractional uncertainty in tropospheric O_3 radiative forcing between the preindustrial and present day, due to rate constant uncertainty. Shown on the left are the 20 most important reactions. 'Other' shows the addition in quadrature of the remaining 40 reactions. 'Total (sum)' indicates the total fractional uncertainty calculated by adding together the individual uncertainties in quadrature. 'ACCMIP' indicates the inter-model spread found from the ACCMIP (Young et al., 2013) study.

Atmos. Chem. Phys. Discuss., doi:10.5194/acp-2017-12, 2017
Manuscript under review for journal Atmos. Chem. Phys.
Discussion started: 9 March 2017

Atmospheric Chemistry and Physics Discussions

Table 1. Table of reactions studied. f (298) indicates the JPL or IUPAC panel uncertainty estimate at 298K and g gives the rate at which this uncertainty increases away from 298K (see previous section). Reactions with 0 for the temperature dependence indicates there is zero temperature dependency or not enough information to provide a temperature varying uncertainty. The final column gives the fractional increase in the ozone burden by increasing the rate constant to its 1σ value. Reactions with a * are the 10 reactions used in the Monte Carlo study.

Number	Reaction	f(298)	g (K)	1σ O_3 burden change (%)
1*	$NO_2 + OH \xrightarrow{M} HNO_3$	1.3	100	-6.20
2*	$OH + CH_4 \rightarrow CH_3O_2 + H_2O$	1.1	100	4.15
3*	$O_3 + NO \rightarrow NO_2 + O_2$	1.1	200	-3.61
4*	$HO_2 + NO \rightarrow NO_2 + OH$	1.15	20	3.09
5*	$O_3 + HO_2 \rightarrow OH + 2O_2$	1.15	80	-2.39
6*	$O(^1D) + N_2 \rightarrow O + N_2$	1.1	20	1.82
7*	$O(^1D) + H_2O \rightarrow OH + OH$	1.08	20	-1.54
8	$HNO_3 + OH \rightarrow H_2O + NO_3$	1.2	0	0.928
9*	$O_3 + NO_2 \rightarrow NO_3 + O_2$	1.15	150	-0.803
10*	$O(^1D) + O_2 \rightarrow O + O_2$	1.1	10	0.745
11	$CH_3C(O)O_2 + NO \rightarrow CH_3O_2 + NO_2 + CO_2$	1.5	0	0.721
12*	$O_3 + OH \rightarrow HO_2 + O_2$	1.15	50	-0.693
13	$CO + OH \rightarrow HO_2 + CO_2$	1.1	100	0.571
14	$CH_3O_2 + NO \rightarrow CH_2O + HO_2 + NO_2$	1.15	100	0.553
15	$CH_3OH + OH \rightarrow HO_2 + CH_2O$	1.1	60	0.462
16	$CH_3C(O)OONO_2 \rightarrow CH_3C(O)OO + NO_2$	1.2	200	0.341
17	$CH_3C(O)O_2 + NO_2 \xrightarrow{M} CH_3C(O)OONO$	1.2	50	-0.289
18	$OH + H_2 \rightarrow H_2O + HO_2$	1.05	100	0.282
19	$OH + H_2O_2 \rightarrow H_2O + HO_2$	1.15	45	0.265
20	$NO + NO_3 \rightarrow 2NO_2$	1.3	100	0.249
21	$HO_2 + NO_3 \rightarrow OH + NO_2$	1.5	0	0.248
22	$CH_3OOH + OH \rightarrow CH_3O_2 + H_2O$	1.4	150	-0.243
23	$CH_3SCH_3 + OH \rightarrow SO_2 + CH_3O_2 + CH_2O$	1.1	100	0.231
24	$OH + HO_2 \rightarrow H_2O + O_2$	1.15	50	-0.215
25	$CH_3CH_2OO + NO \rightarrow CH_3CHO + NO_2 + HO_2$	1.2	150	0.211
26	$C_2H_6 + OH \rightarrow CH_3CH_2OO + H_2O$	1.07	50	0.201
27	$O(^1D) + H_2 \rightarrow OH + H$	1.15	50	0.198
28	$HCOOH + OH \rightarrow H_2O + CO_2 + HO_2$	1.2	100	0.196
29	$OH + OH \rightarrow H_2O + O_3$	1.25	50	0.195
30	$CH_3CHO + NO_3 \rightarrow HNO_3 + CH_3C(O)OO$	1.3	300	0.193

continued on next page

Atmos. Chem. Phys. Discuss., doi:10.5194/acp-2017-12, 2017
Manuscript under review for journal Atmos. Chem. Phys.
Discussion started: 9 March 2017

Atmospheric Chemistry and Physics Discussions

continued from previous page				
31	$HNO_2 + OH \rightarrow H_2O + NO_2$	1.5	200	0.178
32	$CH_3CHO + OH \rightarrow CH_3C(O)OO + CH_2O + CO + HO_2$	1.05	20	0.174
33	$CH_3SCH_3 + NO_3 \rightarrow SO_2 + HNO_3 + CH_3OO + CH_2O$	1.1	150	0.172
34	$CH_3O_2 + CH_3O_2 \rightarrow CH_3OH + CH_2O + O_2$	1.2	100	0.170
35	$HO_2 + HO_2 \rightarrow H_2O_2$	1.15	100	0.166
36	$CH_2O + OH \rightarrow CO + HO_2 + H_2O$	1.15	50	0.156
37	$NO + OH \xrightarrow{M} HNO_2$	1.2	50	-0.151
38	$SO_2 + OH \xrightarrow{M} SO_4 + HO_2$	1.1	100	0.151
39	$NO_2 + NO_3 \xrightarrow{M} N_2O_5$	1.2	100	-0.151
40	$HNO_4 + OH \rightarrow H_2O + NO_2 + O_2$	1.3	500	0.149
41	$OH + OH \xrightarrow{M} H_2O_2$	1.5	100	-0.146
42	$NO_3 + NO_3 \rightarrow 2NO_2 + O_2$	1.5	500	-0.144
43	$OH + NO_3 \rightarrow HO_2 + NO_2$	1.5	0	-0.143
44	$NO_2 + NO_3 \rightarrow NO + NO_2 + O_2$	2	0	-0.134
45	$HNO_4 \rightarrow HO_2 + NO_2$	1.3	100	0.104
46	$HO_2 + NO_2 \xrightarrow{M} HNO_4$	1.1	50	0.0707
47	$CH_3O_3 + HO_2 \rightarrow CH_3OOH + O_2$	1.3	150	0.0350
48	$CH_2{=}C(CH_3)CH{=}CH_2 + OH \rightarrow HOCH_2C(OO)(CH_3)CH{=}CH_2$	1.1	100	-0.0279
49	$NO_3 + CH_2O \rightarrow HNO_3 + HO_2 + CO$	1.3	0	-0.0145
50	$C_4H_{10} + OH \rightarrow 2H_2O + C_4H_9$	1.06	100	0.0132
51	$hv + NO_2 \rightarrow NO + O(^3P)$	1.1	0	2.66
52	$hv + O_3 \rightarrow O_2 + O(^1D)$	1.1	0	-1.97
53	$hv + HNO_3 \rightarrow OH + NO_2$	1.1	0	0.559
54	$hv + CH_2O \rightarrow CO + HO_2 + HO_2$	1.1	0	0.338
55	$hv + HNO_4 \rightarrow HO_2 + NO_2$	1.1	0	0.262
56	$hv + N_2O_5 \rightarrow NO_3 + NO_2$	1.1	0	0.223
57	$hv + NO_3 \rightarrow NO_2 + O(^3P)$	1.1	0	0.222
58	$hv + HNO_4 \rightarrow OH + NO_3$	1.1	0	0.200
59	$hv + CH_3CHO \rightarrow CH_3OO + HO_2 + CO$	1.1	0	0.199
60	$hv + CH_3CHO \rightarrow CH_4 + CO$	1.1	0	0.196